JOURNAL OF MECHANICS OF CONTINUA AND MATHEMATICAL SCIENCES
www.journalimcms.org

ISSN (Online) : 2454 -7190 Vol.-21, No.-06, June (2026) pp 131-141 ISSN (Print) 0973-8975

A COMPARATIVE NUMERICAL STUDY ON COPPER TIN SULPHIDE/SELENIDE BASED SOLAR DEVICE

Srinibas Padhy[1], Biswa Ranjan Swain[2], Sumant Kumar Mohapatra[3] Aditya Acharya[2], Srikanta Kumar Mohapatra[4]

[1]School of Electronics Engineering, KIIT (Deemed to be University), Bhubaneswar, Odisha, India.

[2,4] Department of Electronics and Communication Engineering, Silicon University, Bhubaneswar-751024, Odisha, India.

[3] Department of CSE (AI & ML), School of Engineering, Dayananda Sagar University, Bengaluru-562112, Karnataka, India.

[5]Chitkara University Institute of Engineering & Technology, Chitkara University, Punjab, India.

Email: [1]Srinibas.padhyfet@kiit.ac.in, [2]biswa.iitkgp.ece@gmail.com, [3]sumantkumar-aiml@dsu.edu.in, [4]aditya@silicon.ac.in, [5]srikanta.2k7@gmail.com

Corresponding Author: **Sumant Kumar Mohapatra**

https://doi.org/10.26782/jmcms.2026.06.00007

(Received: March 27, 2026; Revised: May 29, 2026; Accepted: June 10, 2026)

Abstract

SCAPS-1D has been used in this work to model and simulate Copper Tin Sulphide/Selenide (CTS/CTSe) based device numerically. The study focuses on the performance improvement of solar cells made of copper tin sulfide/selenium (CTS/CTSe). Nowadays,CTS/CTSe is labelled as a promising absorber layer, which is analogous to the Kesterite (CZTS) absorber layer. The output parameters are optimized against the variation in Material, Electrical, and Optical parameters. The assumed inputs employed in the numerical simulation are consistent with the practical values. The result demonstrates that by optimization of different layers in the cell, the maximum efficiency of CTS and CTSe obtained are 17.5% and 18.5%, respectively.

Keywords : Numerical Modeling; SCAPS-1D; CTS; CTSe

I. Introduction

Thin film solar cells (TFSC) are renowned for using little material, and hence it involves in low-cost manufacturing process coupled with high efficiency, TFSC materials like Cu(In,Ga)Se2 (CIGS) and Cadmium Teluride (CdTe) have received a lot of interest in research for the past few years. The highest achieved efficiencies are 21% and 23.4%, respectively [VII]. However, due to their toxicity and the scarcity of

indium and gallium, they are not widely used [I,XVIII]. A trustworthy replacement material, such as Copper Tin Sulphide (CTS) and Copper Tin Selenide (CTSe), is being thoroughly investigated as a potential substitute for P-type absorber layer material [VIII,XII]. They resemble CZTS solar cells structurally and feature a bandgap that is extremely near to the ideal single junction value (1.5eV). They are labelled as low-cost, non-toxic substances that are readily available on Earth and can be employed in the solar cell. They are also pivotal material for photovoltaic applications due to their higher absorption coefficient values greater than 105 cm-1. [III,XVII,VI,X]. The primary goal of this study is to conduct a comparative analysis of the CTS/CTSe structure and determine the structure's optimal efficiency. With a bandgap in between 0.5 and 1.5 eV, this CTS structure has an analogous kesterite structure [X]and a high value of absorption coefficient of 105cm-1 [XIV]. The novelty of ongoing numerical modeling work is to get an efficient device by lessening the open-circuit voltage deficit, which is prominent in this kind of solar cell, and finding the best structure depicting the optimized performances. The simulations were run using the SCAPS program [II].

II. Methodology

SCAPS -1D software has been employed in the simulation work. The acronym SCAPS refers to Solar Cell Capacitance Simulator, a tool created at the University of Gent [II].Its primary goal is to ascertain the influence of various features on the device's work under light illumination. The tool with all the simulation features in the current work is the SCAPS-1D program. For CTS and CTSe-based solar cells, the aforesaid software is used to optimize and attain the best efficiency. It has the ability to handle a number of layers with a good user interface and practical scripting facilities[IX].The electron (e-) and hole (e+) continuity equations, as well as the Poisson equation, are all numerically solved by this program. Poisson's formula is shown in Eq. (1), and Eq. (2) explains about Continuity expression.

$$\frac{d}{dx}\left(\varepsilon(x)\frac{d\Psi}{dx}\right) = q[p(x) - n(x) + ND^{+}(x) - NA^{-}(x) + pt(x) - nt(x)] \qquad (1)$$

$$\frac{1}{q}\left(\frac{dJ_{n/p}}{dx}\right) = \pm G_{op}(x) \pm R(x) \qquad (2)$$

The value of electrons and holes $G_{op}(x)$, $R(x)$ are (negative, positive) respectively. The structure is made up of several layers, including the front layer Al:ZnO, the window layer ZnO, the n-typeCdS layer, the absorber layer CTS/CTSe, and the back contact layer Molybdenum. Simulated conditions for the structure are at Air Mass 1.5 and P=1000W/m2. T is set at a fixed temperature of 300K. In Fig.1.aand b, the structures are manifested.The heterostructure consists of AZO/ZnO/CdS/CTS(Mo) and AZO/ZnO/CdS/CTSe(Mo) interfaces. The electron affinity values employed in the SCAPS simulation determine the conduction-band and valence-band alignment across these interfaces. The electron affinity values used for CdS, CTS, and CTSe are 4.4 eV, 4.05 eV, and 4.10 eV, respectively. These values provide favorable carrier transport across the CdS/absorber junction and support efficient carrier extraction.

Although a detailed interface-state analysis is beyond the scope of the present work, the selected parameters are consistent with experimentally reported values and enable realistic numerical modeling of CTS and CTSe solar cells.

Table 1: Material parameters used in the simulation.

Parameters	Al:ZnO	ZnO	CdS	CTS	CTSe	MO
Nomenclature	Front layer	Windo w layer	Buffer layer	Absorber layer	Absorber layer	Back contact
Thickness (nm)	300	50	30	2500	2500	0.61
Electron mobility, μ_n / Hole mobility, μ_p ($cm^2/V\ s$)	100/25	100/25	100/25	100/25	100/12.5	100/25
Acceptor concentration, N_A / Donor concentration, N_D (cm^{-3})	$0/10^{20}$	$0/10^{18}$	$0/1.1\times10^{18}$	10^{16}-$10^{18}/10^{1}$	10^{16}-$10^{18}/10^{3}$	10^{13}-10^{19}
Bandgap, Eg / Electron affinity, χ(eV)	3.3/4.4	3.3/4.4	2.4/4.4	1.5/4.05	1.45/4.1	1.98/4.2 7
Defect density, N_t(cm^{-3})	10^{17}	10^{17}	10^{18}	10^{14}-10^{18}	10^{14}-10^{18}	

III. Layer Optimization

III.iFront, window, and buffer layer property optimization

The structures, shown in **Fig.1.a** and **b**, i.e., CTS and CTSe, have been simulated with the standard practical values exhibited in **Table 1**. The layer optimization was carried out, and the results were shown in the following sections. The top layer of the structure is the Al: ZnO layer. [IV,XIV]. Optimization was accomplished by varying the AZO layer's thickness between 300 and 500 nm. It was noted that the AZO's performance somewhat deteriorates with thickness escalation. The optimized thickness value of 300 was selected. The next layer is the window-functioning ZnO layer. The ZnO layer optimization was carried out by varying the thickness from a value of 50 nm to 110 nm, with 50 nm stated as the ideal thickness. Efficiency decreases as ZnO thickness value rises **[**XIX,XI**]** as the front layer facilitates the passage of sunlight. As a buffer layer, CdS is used. By changing its parameters, the performance can be enhanced. Since the effectiveness slightly decreases as thickness increases, 30 nm was found to be the optimal thickness when the variationis between30 and 100 nm.**[**XIII**]**. Additionally, the simulation's output indicates an improved efficiency relative to concentration for a specified donor concentration of $1.1\times10^{18}cm^{-3}$. N_d is consequently $10^{-18}cm^{-3}$ is taken as the reference value **[**V**]**. The optimization of absorber layers is illustrated in the sections that follow.

III.iiAbsorber layer thickness Optimization

For the purposes of simulation, the overall absorber layer thickness for both CTS and CTSe solar cell structures is considered in accordance with the standard absorber layer thickness of 2500 nm. The thicknesses of both structures were changed, and the results for each value were examined. V_{oc} and J_{sc} for the CTS and CTSe layers are found to be low at lower thickness, which may be due to the increased carrier recombination impact at the interface. As the thickness of the CTS and CTSe layer grows, a lot of electron-hole pairs are created by the absorption of photons, which in turn increases the Jsc and Voc values **[19]**. The value of J_{sc} and V_{oc} increased as a result of the increase in layer thickness, shown in **Tables 2** and **3**.The Jsc value rises as the CTS and CTSe thickness increases from 0.5 to 2.5 um. The efficiency of both cells rises from 500 to 2500 nm in thickness. With more thickness, the efficiency, which is assumed to remain essentially constant, will only marginally rise,as shown in **Fig 2.a** and **b,** and **Fig 3**.**a**and **b** for CTS and CTSe, respectively.

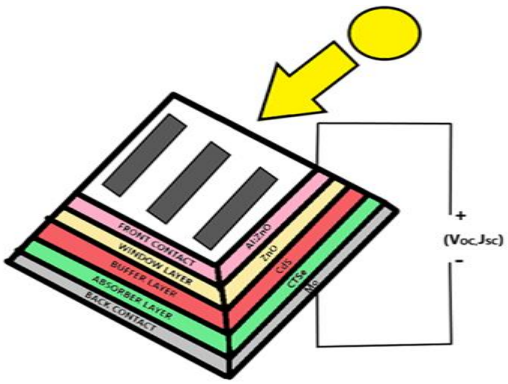

Fig. 1a - CTS solar cell structure

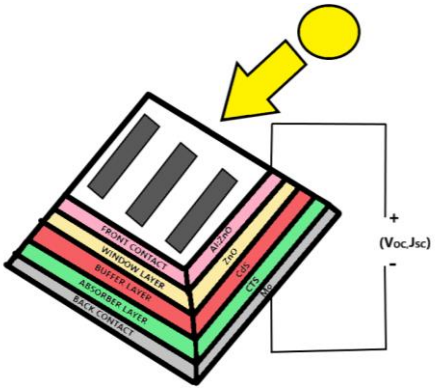

Fig. 1b - CTSe solar cell structure

Table 2: Thickness variation for CTS absorber layer

Thickness(um)	0.5	0.75	1.0	1.25	1.5	1.75	2.0	2.25	2.5
Voc (V)	0.76	0.76	0.76	0.76	0.76	0.76	0.76	0.76	0.76
Jsc (mA/cm2)	23.35	24.78	25.60	26.13	26.5	26.77	26.98	27.14	27.27
FF (%)	78.39	80.34	81.44	82.14	82.63	82.98	83.25	83.46	83.63
Efficiency (%)	13.89	15.16	15.90	16.39	16.73	16.98	17.17	17.32	17.45

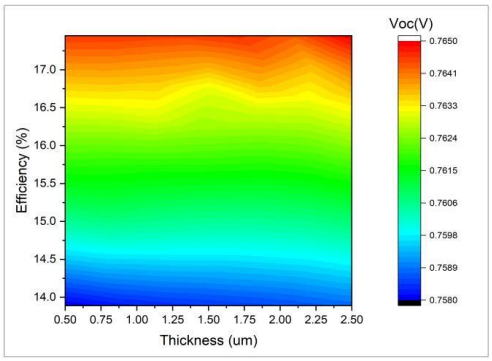

Fig. 2a. Efficiency and Voc contour plot of CTS cell

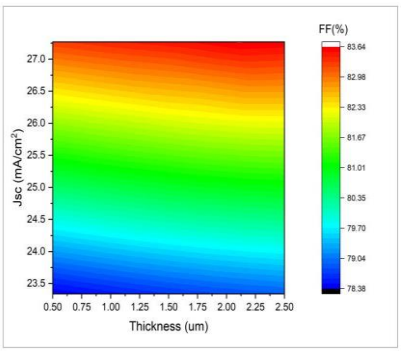

Fig. 2.b. Jsc and fillfactor contour plot of CTS cell

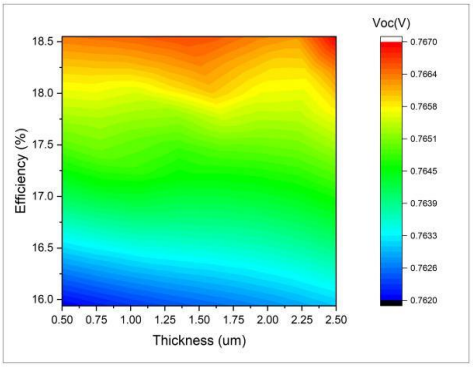

Fig. 3a. Efficiency and Voc contour plot of CTSe cell

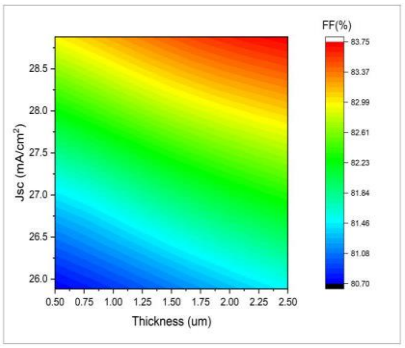

Fig. 3b. Jsc and fillfactor contour plot of CTSe cell

Table 3: Thickness variation for CTSe absorber layer

Thickness(um)	0.5	0.75	1.0	1.25	1.5	1.75	2.0	2.25	2.5
Voc (V)	0.76	0.76	0.76	0.76	0.77	0.77	0.77	0.77	0.77
Jsc (mA/cm2)	25.88	27.05	27.65	28.03	28.3	28.5	28.66	28.78	28.88
FF (%)	80.70	81.57	82.21	82.67	83.00	83.26	83.46	83.62	83.75
Efficiency (%)	15.94	16.86	17.39	17.74	18.00	18.19	18.34	18.45	18.55

III.iii. Optimization of CTS layer properties

III.iii.a. Acceptor concentration Optimization:

The bandgap for copper tin sulphide is considered to be 1.5 eV, which corresponds to the electron affinity value of 4.05 eV. The role of acceptor concentration is investigated.The graphs**Fig.4.a** and **b** show that as acceptor concentration increases, the V_{OC} value improves between 10^{16} $cm^{-3}$and 10^{18} cm^{-3}, which was considered as the acceptor concentration range,and the value of 10^{18} cm^{-3} was selected. As it is pertinent to explain that the more the concentration more the ions, which in turn contribute to the field to migrate the carriers upon illumination **[XIII]**.

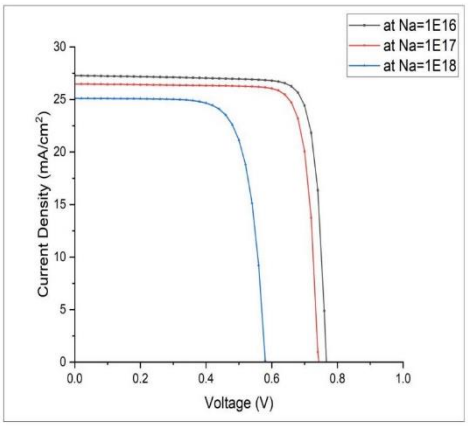

Fig.4a. JV curve of CTS as a function of N_a

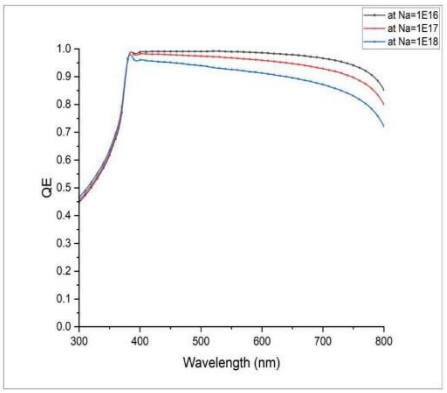

Fig.4b. Quantum Efficiency curve of CTS as a function of N_a

III.iii.b. Defect Density Optimization

Defect density was measured between 10^{14c}m-3 and 10^{18}cm^{-3}. Recombination causes the efficiency to drop with an increase in defect density. The V_{OC}, J_{SC}, FF, and Efficiency values decrease, attributed to the increased number of recombination centres **[20]**. After running the simulations, the ideal value for $N_t$was determined to be 10^{14} cm^{-3}. Fig. **5.a.** depicts the JV curve. The QE curve is shown in **Fig.5.b.**

III.iv.a. Acceptor concentration Optimization

With a direct optical bandgap between 1.1 and 1.7 eV **[XII]** and an electron affinity of 4.1 eV. Variation of acceptor concentration of CTSe layer exhibits a change in output values. The fill factor and efficiency increase as a result of the V_{OC} and J_{SC} values improving, which may be attributed to enhanced ions that drift the carriers more profoundly. The range was selected 10^{16} cm^{-3} to 10^{18} cm^{-3},which is consistent with practical values, and an optimized value of N_a 10^{16} cm^{-3} was selected (depicted in **Fig.6.a** and **b**)

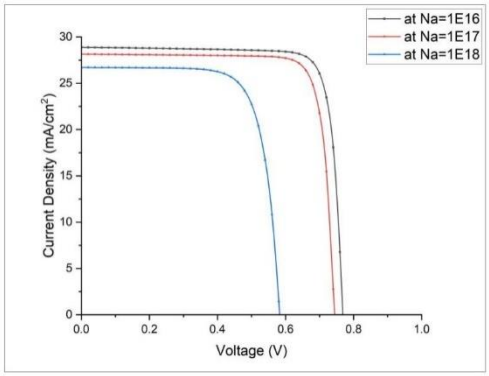

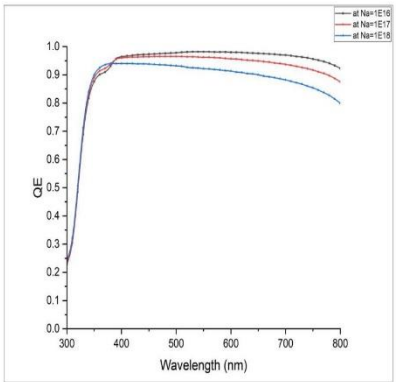

Fig.6a. JV curve of CTSe as a function of N_a**Fig.6b.** Quantum Efficiency curve of CTSe as afunction of N_a

III.iv.b. Defect Density Optimization:

It has been noted that characteristics, including V_{OC}, J_{SC}, FF, and efficiency, decrease with an increase in defect density. As it's clear that the higher the defect density, the more the loss due to the recombination process **[XX]**. The defect density variation range has been taken in accordance with the practical values. It has been reported that the best efficiency is obtained at $N_t=10^{14}cm^{-3}$. **Fig. 7.a.** exhibits the JV curve, **Fig. 7.b**.the QE curve.

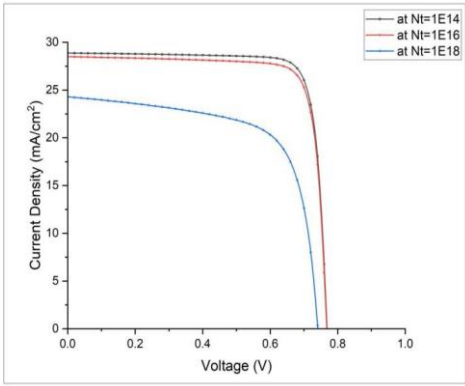

Fig.7a. JV characteristics curve of CTS as a function of N_t

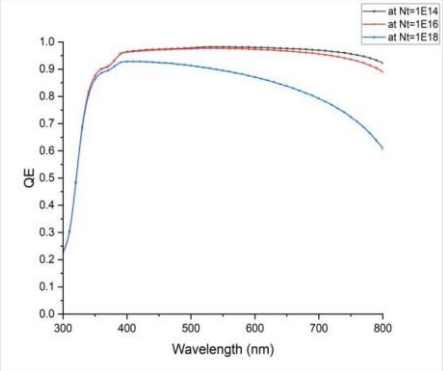

Fig.7b. Quantum Efficiency curve of CTSe as a function of N_t

III.iv.c. Voltage Deficit and Recombination Analysis

The open-circuit voltage deficit (V_{def}) is an important parameter for evaluating photovoltaic losses and is defined as:

$$V_{def}=Eg/q-V_{oc}$$

For the optimized CTS device having Eg=1.50 eV and V_{oc}=0.76V, the calculated voltage deficit is 0.74 V. Similarly, for the optimized CTSe device with Eg=1.45 eV and Voc=0.77V, the voltage deficit is found to be 0.68 V.

The lower voltage deficit observed in CTSe indicates comparatively lower recombination losses. Furthermore, the defect density optimization results presented in Sections 3.3.2 and 3.4.2 reveal that an increase in defect density from 10^{14} to 10^{18} cm^{-3} significantly reduces Voc, Jsc, FF, and efficiency. This behavior confirms that defect-assisted Shockley-Read-Hall recombination is one of the dominant loss mechanisms in both CTS and CTSe devices.The comparatively better performance of CTSe may therefore be attributed to its lower recombination sensitivity and improved carrier collection capability.

III.iv.d. Comparative Analysis of CTS and CTSe Absorbers

Although CTS and CTSe possess similar crystal structures, selenium substitution significantly influences the electronic and optical properties of the absorber layer. CTSe exhibits a slightly lower bandgap (1.45eV) compared with CTS (1.50eV), which enables absorption of longer wavelength photons and consequently improves photogenerated carrier concentration.The simulation results demonstrate that

CTSeconsistently produces higher short-circuit current density and efficiency than CTS. The optimized CTSe device achieves a Jsc of 28.88 mA/cm² and efficiency of 18.55%, whereas CTS provides 27.27 mA/cm² and 17.45%, respectively.In addition, CTSe shows lower voltage deficit and reduced sensitivity to recombination losses. Therefore, selenium incorporation contributes to enhanced carrier transport and carrier generation, leading to superior photovoltaic performance.

III.v. Optimum CTS/CTSe device characteristics

With the aforesaid device layer properties, the optimum CTS and CTSedevices are found with efficiency of 17.5 and 18.5%,respectively, as shown in **Fig.8.a** and **b**.

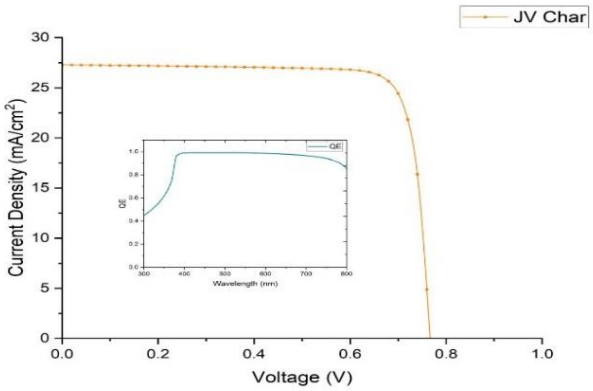

Fig. 8a. JV characteristics of CTS device

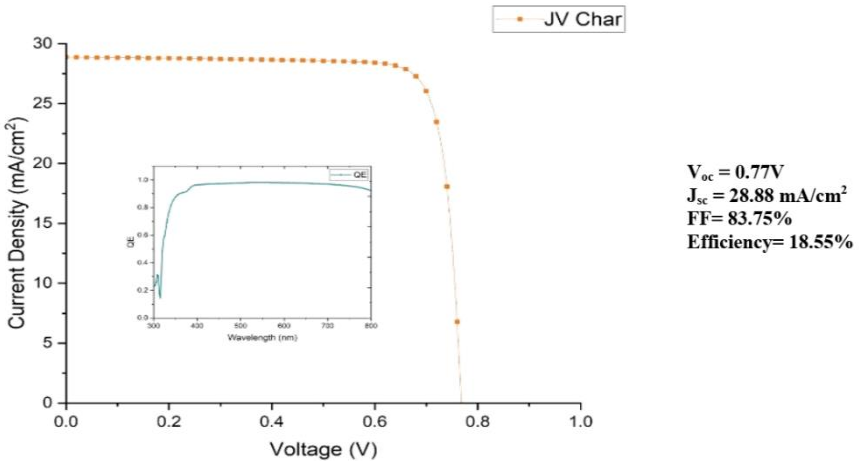

Fig. 8b. JV characteristics of CTSe device

IV. Conclusion

The present study demonstrates the comparative numerical analysis of CTS vis-à-vis CTSe absorber layer with the aid of SCAPS-1D software. By tweaking the material, electrical, and optical parameters, the obtained efficiencies pertaining to CTS and CTSe obtained are 17.5% and 18.5%, respectively. It has been found that the properties of the absorber layer have a predominant impact on device output performance compared to other layers in the device. The numerical study gives a meaningful impetus to the material scientist to fabricate CTS and CTSe-based solar devices.

Conflict of Interest:

The authors declare that there was no relevant conflict of interest regarding this paper.

References

I. Andersson, B. A. "Materials Availability for Large-Scale Thin-Film Photovoltaics." Progress in Photovoltaics: Research and Applications, vol. 8, no. 1, 2000, pp. 61–76. 10.1002/(SICI)1099-159X(200001/02)8:1<61::AID-PIP301>3.0.CO;2-6.

II. Burgelman, Marc, Koen Decock, Alex Niemegeers, Johan Verschraegen, and Stefaan Degrave. SCAPS Manual. University of Gent, 2021. URL: https://scaps.elis.ugent.be/SCAPS%20manual%20most%20recent.pdf.

III. Chierchia, R., et al. "Properties of Copper Tin Sulphide Thin Films for Photovoltaic Applications." Physica Status Solidi C, vol. 13, no. 1, 2016, pp. 35–40. 10.1002/pssc.201510214.

IV. Dubey, P. K., and V. V. Paranjape. "Open-Circuit Voltage of a Schottky-Barrier Solar Cell." Journal of Applied Physics, vol. 48, 1977, pp. 324–328. 10.1063/1.323560.

V. Et-taya, L., T. Ouslimane, and A. Benami. "Numerical Analysis of Earth-Abundant $Cu_2ZnSn(SxSe1-x)_4$ Solar Cells Based on Spectroscopic Ellipsometry Results by Using SCAPS-1D." Solar Energy, vol. 201, 2020, pp. 827–835. 10.1016/j.solener.2020.03.056.

VI. Fernandes, P., P. Salomé, and A. da Cunha. "Study of Cu_2SnS_3 Thin Films for Solar Cell Applications." Journal of Physics D: Applied Physics, vol. 43, no. 21, 2010, p. 215403. 10.1088/0022-3727/43/21/215403.

VII. Green, Martin A., et al. "Solar Cell Efficiency Tables." Progress in Photovoltaics: Research and Applications, vol. 27, no. 1, 2019. 10.1002/pip.3102.

VIII. Hossain, E. S., et al. "Copper Tin Sulphide Thin Films for Photovoltaic Applications." Current Applied Physics, vol. 18, no. 1, 2018, pp. 79–89. 10.1016/j.cap.2017.11.001.

IX. Khoshsirat, N., and N. A. Md Yunus. "Numerical Simulation of CIGS Thin Film Solar Cells Using SCAPS-1D." IEEE Conference on Sustainable Utilization and Development in Engineering and Technology, 2013. URL: https://ieeexplore.ieee.org/

X. Kuku, T. A., and O. A. Fakolujo. "Optical Properties of Copper Tin Sulphide Thin Films." Solar Energy Materials, vol. 16, no. 1, 1987, pp. 199–205. URL: https://www.sciencedirect.com/

XI. Kamal, M. M., and Mia. "Optimization of Linear Antenna Array Thinning Using Binary Genetic Algorithm (BGA)." 2022 International Conference on Recent Trends in Information Technology (ICRITO), IEEE, 2022, 10.1109/ICRITO56286.2022.9964507.

XII. Pallavolu, Mohan Reddy, et al. "Status Review on Cu_2SnSe_3 (CTSe) Thin Films for Photovoltaic Applications." Solar Energy Materials and Solar Cells, vol. 208, 2020. 10.1016/j.solmat.2020.110367.

XIII. Peijie, L., et al. "Numerical Simulation of Cu_2ZnSnS_4-Based Solar Cells with In_2S_3 Buffer Layers by SCAPS-1D." Journal of Applied Science and Engineering, vol. 17, no. 4, 2014, pp. 383–390. URL: http://jase.tku.edu.tw/

XIV. Rahaman, Sabina, et al. "Effect of Copper Concentration on CTS Thin Films for Solar Cell Absorber Layer and Photocatalysis Applications." Materials Science in Semiconductor Processing, vol. 145, 2020, Article 106589. 10.1016/j.mssp.2020.106589.

XV. Rahman, M. A. "Enhancing the Photovoltaic Performance of Cd-Free Cu_2ZnSnS_4 Heterojunction Solar Cells Using SnS HTL and TiO_2 ETL." Solar Energy, vol. 215, 2021, pp. 64–76. 10.1016/j.solener.2020.12.058.

XVI. Rui, K., et al. "New World Record CIGSSe Thin-Film Solar Cell Efficiency Beyond 22%." IEEE 43rd Photovoltaic Specialists Conference, 2016. URL: https://ieeexplore.ieee.org/

XVII. Sato, S., et al. "Properties of Cu_2SnSe_3 Thin Films for Photovoltaic Applications." Physica Status Solidi C, vol. 12, no. 6, 2015, pp. 757–761. 10.1002/pssc.201510040.

XVIII. Schubert, B.-A., et al. "Advances in Thin-Film Photovoltaic Technologies." Proceedings of the 23rd European Photovoltaic Solar Energy Conference, Valencia, 2008. URL: https://www.eupvsec-proceedings.com/

XIX. Simya, O. K., A. Mahaboobbatcha, and K. Balachander. "A Comparative Study on the Performance of Kesterite-Based Thin Film Solar Cells Using SCAPS Simulation Program." Superlattices and Microstructures, vol. 82, 2015, pp. 248–261. 10.1016/j.spmi.2015.02.029.

XX. Zhao, W., W. Zhou, and X. S. Miao. "Numerical Simulation of CZTS Thin Film Solar Cell." IEEE NEMS Conference, 2012. 10.1109/NEMS.2012.6196826.